The First Strain of *Clostridium perfringens* Isolated from an Avian Source Has an Alpha-Toxin with Divergent Structural and Kinetic Properties[†,‡]

Neil Justin,[§,||] Nicola Walker,[⊥] Helen L. Bullifent,[⊥] Glenn Songer,[@] Dawn M. Bueschel,[@] Helen Jost,[@] Claire Naylor,[§] Julie Miller,[⊥] David S. Moss,[§] Richard W. Titball,[⊥,#] and Ajit K. Basak*[,§]

School of Crystallography, Birkbeck College, Malet Street, London WC1E 7HX, United Kingdom, Defence Science and Technology Laboratory, CBS Porton Down, Salisbury, Wiltshire SP4 0JQ, United Kingdom, Department of Veterinary Science, University of Arizona, Tucson, Arizona 85721, and Department of Infectious and Tropical Diseases, London School of Hygiene and Tropical Medicine, Keppel Street, London WC1E 7HT, United Kingdom

Received November 2, 2001; Revised Manuscript Received February 11, 2002

ABSTRACT: *Clostridium perfringens* alpha-toxin is a 370-residue, zinc-dependent, phospholipase C that is the key virulence determinant in gas gangrene. It is also implicated in the pathogenesis of sudden death syndrome in young animals and necrotic enteritis in chickens. Previously characterized alpha-toxins from different strains of *C. perfringens* are almost identical in sequence and biochemical properties. We describe the cloning, nucleotide sequencing, expression, characterization, and crystal structure of alpha-toxin from an avian strain, SWan *C. perfringens* (SWCP), which has a large degree of sequence variation and altered substrate specificity compared to these strains. The structure of alpha-toxin from strain CER89L43 has been previously reported in open (active site accessible to substrate) and closed (active site obscured by loop movements) conformations. The SWCP structure is in an open-form conformation, with three zinc ions in the active site. This is the first example of an open form of alpha-toxin crystallizing without the addition of divalent cations to the crystallization buffer, indicating that the protein can retain three zinc ions bound in the active site. The topology of the calcium binding site formed by residues 269, 271, 336, and 337, which is essential for membrane binding, is significantly altered in comparison with both the open and closed alpha-toxin structures. We are able to relate these structural changes to the different substrate specificity and membrane binding properties of this divergent alpha-toxin. This will provide essential information when developing an effective vaccine that will protect against *C. perfringens* infection in a wide range of domestic livestock.

Alpha-toxin from *Clostridium perfringens* was the first bacterial protein shown to possess both enzymatic and toxic properties (*1*). It is a zinc metalloenzyme (*2*) and is composed of 370 residues. Alpha-toxin is a phospholipase C (PLC)[1] and exhibits hemolytic, necrotic, vascular permeabilization, and platelet aggregating properties (*3*). It is predominantly associated with the disease gas gangrene in humans (*4*). However, alpha-toxin has also been implicated in the pathogenesis of sudden infant death syndrome in humans (*5*) and in animals (*6*) and with necrotic enteritis in chickens (*7*, *8*). Necrotic enteritis is a serious and often fatal disease, which can increase in incidence when antibiotic growth promoters are withdrawn from feedstuff (*9*). The toxicity of alpha-toxin is a consequence of the hydrolysis of cell membrane phospholipids, as the diacylglycerol products cause the perturbation of cell metabolism resulting in the activation of the arachidonic acid cascade and protein kinase C (*3*). More extensive hydrolysis of membrane phospholipids can result in target cell lysis. The alpha-toxin encoding genes from several strains of *C. perfringens* have previously been isolated and characterized (*10*), and the encoded proteins are highly conserved with the sequences only differing by approximately 1.5% overall.

The structure of alpha-toxin from a bovine isolate of *C. perfringens* (strain CER89L43) has previously been determined in two different conformations (*11*, *12*). The enzyme consists of two domains. The N-terminal domain (residues 1−246) is α-helical and contains the active site, which is indicated by the presence of either two or three metal ions. In the first of the two structures (the open form) which was crystallized in the presence of 50 mM cadmium (a zinc and calcium ion analogue), the active site of the enzyme was accessible for substrate binding and contained all three metal ions essential for activity (*11*). In the second structure (the

[†] We thank the BBSRC for their financial support. N.J. thanks the BBSRC and Dstl for the BBSRC-CASE studentship which supported him during this work.

[‡] Coordinates have been deposited in the Protein Data Bank as entry 1KHO.

* To whom correspondence should be addressed. E-mail: a.basak@mail.cryst.bbk.ac.uk. Telephone: +4420 7631 6823.

[§] Birkbeck College.

[||] Current address: Division of Protein Structure, National Institute for Medical Research, The Ridgeway, Mill Hill, London NW7 1AA, U.K.

[⊥] Defence Science and Technology Laboratory.

[@] University of Arizona.

[#] London School of Hygiene and Tropical Medicine.

[1] Abbreviations: PLC, phospholipase C; PCR, polymerase chain reaction; EYU, egg yolk units; ρNPPC, *p*-nitrophenylphosphorylcholine; rms, root-mean-square.

10.1021/bi012015v CCC: $22.00
Published on Web 04/26/2002

closed form; *12*), which was crystallized in the absence of any divalent cations, two mobile loops (residues 55−93 and 132−149) had altered conformations which obscured the active site. In addition, the movement of these loops had destroyed one of the three metal ion binding sites so that this form of the enzyme contained just two zinc ions in the N-terminal domain.

The C-terminal domain, which is known to be essential for toxicity (*13*, *14*), is an eight-stranded β-sandwich, structurally analogous to the calcium- and membrane-binding eukaryotic C2 domains (*15*). We have previously shown that calcium binds to loops at the top of this domain (*16*), and it has been shown by us and others that the mutation of residues essential for this calcium binding reduces the activity of the protein (*17*, *18*). In addition, a surface containing the active site cleft in the N-terminal domain and the three calcium-binding sites of the C-terminal domain, together with a number of exposed hydrophobic residues, has been identified; we have proposed this surface to be the membrane-binding plane of the molecule (*11*, *16*).

Alpha-toxin is known to hydrolyze the phospholipid substrates phosphatidylcholine and sphingomyelin (*19*, *20*), both of which are key components of the outer leaflet of eukaryotic cell membranes. The alpha-toxins characterized to date have similar activities toward these substrates and similar hemolytic activities (*10*). However, related phospholipase C enzymes (collectively with alpha-toxin termed the zinc metallophospholipases C) from other species of bacteria have markedly different properties (*2*). For example, the *Clostridium bifermentans* PLC is significantly less active than alpha-toxin on phosphatidylcholine or sphingomyelin liposomes and is more than 100-fold less hemolytic and only weakly toxic (*21*). The *Bacillus cereus* PLC, which lacks a C-terminal domain, is not hemolytic or toxic.

In this paper, we describe the cloning, expression, purification, characterization, and crystal structure of alpha-toxin from an avian isolate of *C. perfringens* (strain SWCP). This strain was isolated from a swan that had died from an intestinal *C. perfringens* infection resulting in extensive mucosal necrosis and hemorrhage. The SWCP alpha-toxin exhibited a large degree of sequence variation compared to the previously characterized *C. perfringens* alpha-toxins and had altered substrate specificity (*10*). We have identified regions in the crystal structure of the SWCP alpha-toxin that were different from the previously reported crystal structures of alpha-toxins (*11*, *12*). One of the regions of dissimilarity was the membrane binding region formed by C-terminal residues 330−338, which had previously been shown to bind neutralizing monoclonal antibodies (*10*). Vaccines and antitoxins have been proposed for the prevention and treatment of diseases caused by alpha-toxin. The structural and sequence information provided here could ensure that such vaccines and antitoxins have a broad spectrum of activity.

MATERIALS AND METHODS

Chemicals and Enzymes. Unless otherwise stated, all chemicals and enzymes were obtained from Sigma-Aldrich (Poole, U.K.) or from Roche Molecular Biochemicals (Lewes, U.K.).

Strain Identification and Isolation of DNA. An anaerobic culture was isolated from the intestinal tract of a dead male white swan, which had apparent dehydration, weight loss, and diarrhea. Isolated bacteria were analyzed using the PCR genotyping for the alpha-toxin (*cpa*) and theta-toxin (*pfo*) genes. Chromosomal DNA was isolated from *C. perfringens* strain SWCP according to the method of van Damme-Jongsten (*22*).

Amplification and Cloning of the cpa Gene from C. perfringens. A DNA fragment which would encode the strain SWCP *cpa* ORF was generated using the PCR. The oligonucleotides were designed from the strain NCTC8237 *cpa* gene nucleotide sequence (GenBank accession number X13608). The oligonucleotides 5′ GCT TGG GGC CCA GTG CAA GTG TTA ATC GTT AT 3′ and 5′ TGC TCT AGA GTA AAT ACC ACC AAA ACC AAT 3′, which incorporated *Dra*II and *Xba*I restriction endonuclease sites, respectively, were used during 30 cycles of PCR (96 °C for 30 s, 45 °C for 30 s, and 72 °C for 30 s; Perkin-Elmer 9600 GeneAmp PCR System from PE Applied Biosystems, Warrington, U.K.). The reaction products were purified, digested with the appropriate enzymes, and ligated with suitably digested plasmid α prom27. The α prom27 plasmid was prepared (H. L. Bullifent, unpublished results) by insertion of a *C. perfringens cpa* promoter into plasmid pBluescript II KS (+) (Stratagene Europe, Amsterdam, The Netherlands). After transformation into *Escherichia coli* BL21 cells by electroporation (*23*), bacteria containing the *cpa* gene were identified by the presence of a zone of turbidity surrounding colonies on L-agar containing ampicillin and egg yolk (*24*).

Nucleotide Sequencing. Plasmid DNA was prepared using the Midi plasmid kit (Qiagen Ltd., Crawley, U.K.). DNA sequencing was performed by Oswel DNA Services (Southampton, U.K.). Sequencing primers were designed using the strain NCTC8237 *cpa* gene nucleotide sequence. Forward primers 5′ TCT TAT TCC ATA CCA GAT AC 3′, 5′ AAT ATA CTA TAG TCA TGC 3′, and 5′ TTG ACG ATA TAC AAA ATA TG 3′ bound to the ORF starting at nucleotides 344, 690, and 1036, respectively. Forward primer 5′ AAT TAA CCC TCA CTA AAG GG 3′ bound to the T3 promoter site on the pBluescript II KS (+) plasmid. Reverse primers 5′ AAG ATC ATG CAT GTT CTG 3′, 5′ AAC CGC AGT TAC GTT AGC 3′, and 5′ TAT ATG TAC CCA GAT GTT C 3′ bound to the ORF starting at nucleotides 228, 514, and 795, respectively. Reverse primer 5′ GTA ATA CGA CTC ACT ATA GGG C 3′ bound to the T7 promoter site on the pBluescript II KS (+) plasmid. Three independently obtained plasmids containing the cloned SWCP *cpa* gene were nucleotide sequenced and found to be identical. The nucleotide sequence of the SWCP *cpa* gene has been deposited with GenBank under accession number AF204209.

Purification of Alpha-Toxin. The alpha-toxin was purified from the periplasmic fraction of *E. coli* (*24*) containing the cloned *cpa* gene from *C. perfringens* strain SWCP. The toxin was purified using a modified version of the protocol described previously by Basak et al. (*25*); two stages of ion-exchange chromatography, a Q-Sepharose column (Amersham-Pharmacia Biotech UK Ltd., Little Chalfont, U.K.) followed by a MonoQ column (Pharmacia Biotech), were used.

Measurement of Phospholipase C and Hemolytic Activities. Phospholipase C activity was measured by a microtiter assay using egg yolk phospholipids, phosphatidylcholine

liposomes, sphingomyelin liposomes, or *p*-nitrophenylphosphorylcholine (ρNPPC) as the substrate (*24*). The end point for these assays was determined as the reciprocal of the dilution resulting in 50% activity after incubation at 37 °C for 1 h. The egg yolk assay used the supernatant from egg yolk emulsion (Oxoid Ltd., Basingstoke, U.K.), and the absorbency was measured at 540 nm and the activity expressed in egg yolk units (EYU). Phosphatidylcholine and sphingomyelin liposomes were prepared using the procedure reported by Senior et al. (*26*). After incubation, the activity was measured by the release of fluorescent carboxyfluorescein from the liposomes (excitation wavelength of 485 nm and emission at 520 nm). The activity was expressed as the concentration of alpha-toxin (micrograms per milliliter) that caused 50% lysis. Cleavage of ρNPPC by alpha-toxin resulted in the release of ρ-nitrophenol, which was assessed spectrophotometrically at 414 nm. Activity was expressed in units per milligram where 1 unit hydrolyzes 1 nmol of ρNPPC in 1 min at 37 °C. Hemolytic activity was measured using a microtiter tray assay with 5% (v/v) washed mouse red blood cells (*24*); the 50% hemolysis end point was determined, and activity was expressed as hemolytic units (HU). The alpha-toxin from strain NCTC8237 was used as a control for all the tests; it is known to have enzymatic, hemolytic, and toxic properties similar to those of the strain CER89L43 alpha-toxin (*10*).

Crystallization. Crystals of *C. perfringens* strain SWCP alpha-toxin were grown by hanging drop vapor diffusion at 4 °C. Crystals grew in the presence of 0.5 M sodium acetate, 6−10% 2-propanol or acetone, and 0.1 M sodium cacodylate at pH 6.5. Each drop contained 1.5 μL of protein at 10 mg/mL in 10 mM Tris-HCl (pH 8.0) and 1.5 μL of well buffer. The better diffraction quality crystals were grown in acetone.

X-ray Data Collection. Data were collected from cryocooled crystals following immersion in mother liquor containing 30% (v/v) glycerol as a cryoprotectant [using the procedure described by Garman and Schneider (*27*)]. The data were collected on stations 7.2 and 9.6 of the Synchrotron Radiation Source at Daresbury Rutherford Appleton Laboratory (Warrington, U.K.) on a 300 mm MarResearch Image-Plate and an ADSC Quantum4 CCD detector, respectively. All data were processed with the HKL program suite (*28*). Scaling and merging were performed using the CCP4 program SCALA (*29, 30*). Subsequent data manipulation used the CCP4 program package (*29*). Statistics for the data are given in Table 1. The symmetry of the crystals was found to be $P4_122$ or $P4_322$ with the following unit cell dimensions: $a = b = 117.2$ Å, $c = 220.6$ Å, and $\alpha = \beta = \gamma = 90°$. The Matthew's coefficient (and solvent content) for two, three, and four molecules was 4.8 (73.9%), 3.2 (60.9%), and 2.4 Å^3/Da (47.9%), respectively, but no noncrystallographic self-rotation function peaks could be identified.

Molecular Replacement. Molecular replacement was carried out using the AMoRe package (*31*), with two, three, and four molecules in the asymmetric unit, and in both possible space groups. The open form of alpha-toxin (*11*), with the modeled, disordered loop (residues 84−91) removed and the amino acids that differed between the two sequences replaced with alanine residues, was used as the model. The best solution was for space group $P4_122$ and two molecules in the asymmetric unit, with a correlation coefficient of 64.1% and an *R*-factor of 37.3%. For comparison, the correlation coefficient and *R*-factor were 33.3 and 49.2%, respectively, for two molecules in $P4_322$. It was not possible to place any further copies of the model in the asymmetric unit. We therefore concluded that the correct space group was $P4_122$ with two molecules in the asymmetric unit. Following initial rigid body refinement of this solution, the *R*-factor and R_{free} were 36.4 and 37.5%, respectively.

Table 1: Data Collection and Refinement Statistics

	Data Collection	
resolution range (Å)	30−2.4	
no. of observations	1381901 (measured)[a]	59496 (unique)
completeness (%)	97.8 (all data)	91.3 (2.53−2.4 Å)
R_{merge} (%)[b]	5.7 (all data)	18.7 (2.53−2.4 Å)
$I/\sigma(I)$	25.6 (all data)	6.8 (2.53−2.4 Å)

	Refinement	
	number	average B (Å^2)
protein non-H atoms	5990	33.1 (MC) 34.3 (SC)
zinc ions	6	27.0
water molecules	152	38.1
R (%)[c]	20.6	
R_{free} (%)[d]	24.2	
rmsds	0.01 Å (bonds)	1.88° (angles)

[a] Includes a low-resolution data collection pass (30−3.0 Å). [b] $R_{merge} = \sum|I_I - I_m|/\sum I_m$, where I_I and I_m are the observed intensity and mean intensity of related reflections, respectively. [c] $R = \sum|F_{obs} - F_{calc}|/\sum F_{obs}$ for the 92% of the data included in the refinement. [d] $R_{free} = \sum|F_{obs} - F_{calc}|/\sum F_{obs}$ for the 8% of the data randomly selected and excluded from refinement. MC, main chain; SC, side chain.

Density Modification. Noncrystallographic averaging, solvent flattening, and histogram modification were carried out using the program DM (*32*), prior to the calculation of SigmaA weighted maps (*33*) for manual rebuilding of the model.

Model Building and Refinement. Manual model building was performed using the program O (*34*). The refinement was performed using X-PLOR, version 3.851 (*35*). Alanine residues in the model used for molecular replacement were changed to the correct SWCP amino acid when positive difference Fourier density could be seen. Zinc ions were placed in the active site after the identification of clear positive peaks in the difference map. A bulk solvent correction ($k = 0.35$ and $B = 63.2$ Å^2) was made following the fitting of all amino acids in the SWCP sequence. Noncrystallographic symmetry restraints were used throughout refinement, except in the later stages where there was clear evidence in the calculated electron density map indicating a difference between the two molecules in the asymmetric unit. Water molecules were added to the model at the end of refinement, where there was a 3 rms peak in the difference density and a 1 rms peak in the $2F_o - F_c$ map. Refinement was ended when the *R*-factor and R_{free} had apparently converged at 20.7 and 24.2%, respectively.

RESULTS

Isolation of C. perfringens SWCP from a Swan Suffering from Necrotic Enteritis. C. perfringens strain SWCP was isolated from a male swan, which had been suffering from apparent dehydration, weight loss, and diarrhea. Gross examination of the small and large intestine revealed extensive mucosal necrosis and hemorrhage, with necrotic casts adherent to the ulcerated mucosa. The terminal large intestine contained a pseudomembranous necrotic cast.

Microscopically, sections of the large and small intestine had severe superficial necrotizing and hemorrhagic enteritis. Bacteria were present in extensive pools of necrotic cellular debris. The lamina propria was edematous and congested. Multifocal mucosal erosion, ulceration, hemorrhage, and intestinal edema were evident. These lesions were consistent with clostridial necrotic enteritis, and anaerobic culture of the intestinal tract yielded *C. perfringens*.

The cpa Gene in C. perfringens Strain SWCP Encodes a Sequence-Divergent Form of Alpha-Toxin. The *cpa* gene from *C. perfringens* strain SWCP was amplified using PCR from strain SWCP DNA. The amplified gene was cloned and nucleotide sequenced. Like alpha-toxin from *C. perfringens* strain NCTC8237 (strain originally isolated from an infected wound) or alpha-toxin from *C. perfringens* strain CER89L43 (strain originally isolated from the gut of a diseased calf), the SWCP *cpa* gene encodes a 398-amino acid protein. The first 28 amino acids formed a signal sequence. The relative molecular mass of the mature SWCP alpha-toxin, after removal of the signal sequence, was calculated to be 42 372 Da with an isoelectric point of 4.9, and there are 57 and 58 amino acid differences from the NCTC8237 and CER89L43 alpha-toxins, respectively (Figure 1). SWCP alpha-toxin has a smaller number of charged residues in comparison with the NCTC8237 and CER89L43 alpha-toxins: there are 59 and 54 acidic and basic residues, respectively, in CER89L43 alpha-toxin, whereas there are only 55 acidic and 48 basic residues in the SWCP protein. The number of large hydrophobic residues was similar in all three proteins. However, the SWCP alpha-toxin contained a larger number of polar residues than the NCTC8237 or CER89L43 alpha-toxins (*10*). The SWCP alpha-toxin also differs from the previously reported most divergent forms of alpha-toxin, encoded by the *cpa* genes in *C. perfringens* strains 8-6 and NCIB10662, and from the *C. bifermentans* and *Clostridium novyi* phospholipases C (Figure 1).

The strain SWCP *cpa* gene was cloned into a plasmid, downstream of the strain NCTC8237 *cpa* gene promoter, and expressed in *E. coli*. Protein was isolated from the periplasmic space of the recombinant *E. coli* (*25*) and purified using ion-exchange chromatography. SWCP alpha-toxin purified in this way was judged to be >95% pure when analyzed by SDS−PAGE with a yield of 6.8 mg of purified protein from 1 L of culture.

The Phospholipase C and Hemolytic Activities of the SWCP and NCTC8237 Alpha-Toxins Are Dissimilar. There were differences between the enzymatic and hemolytic activity of the SWCP alpha-toxin and the NCTC8237 alpha-toxin (Figure 2). The NCTC8237 toxin exhibited a slightly higher rate of activity than the SWCP alpha-toxin when egg yolk or sphingomyelin liposomes were used as the substrates. However, when tested with phosphatidylcholine liposomes, the SWCP alpha-toxin was 12 times more active than the strain NCTC8237 alpha-toxin. In contrast, the NCTC8237 alpha-toxin was 4.5 times more hemolytic than the SWCP alpha-toxin and more than 8 times more active when tested toward the synthetic substrate *ρ*NPPC. For the NCTC8237 alpha-toxin, these results were similar to previously reported data (*24*). Overall, the results show that both the SWCP and NCTC8237 alpha-toxins have high PLC activity, but that variations in substrate specificity have been caused by the large number of amino acid changes between the two strains.

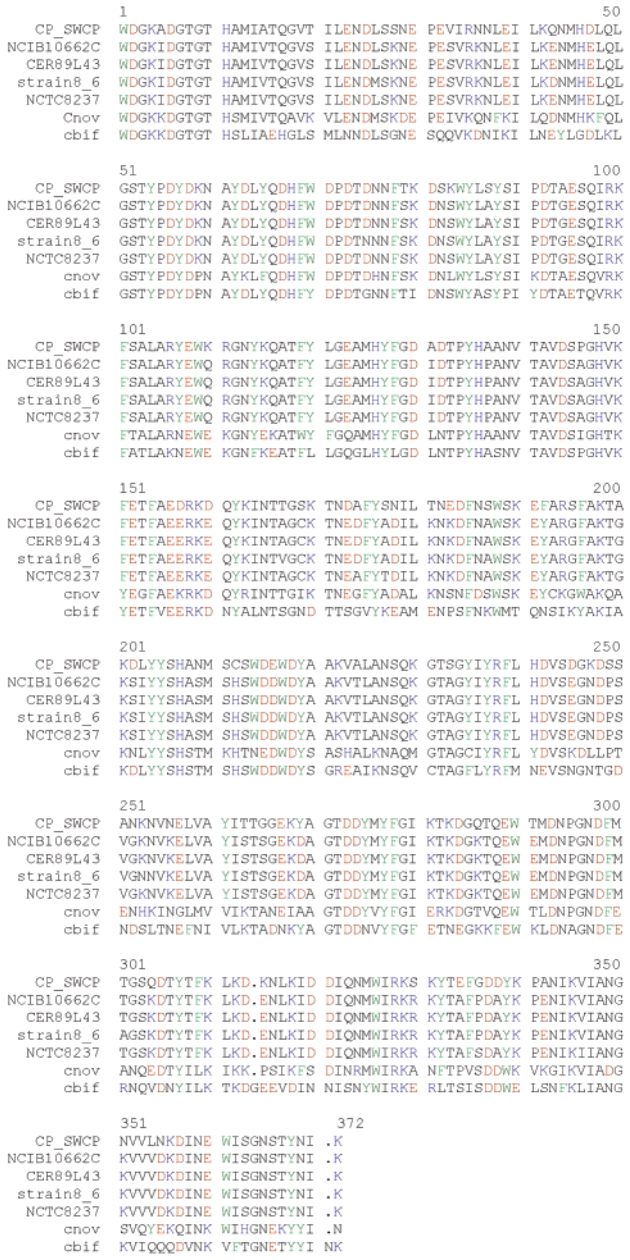

FIGURE 1: Amino acid alignment of related bacterial phosphatidylcholine-specific phospholipases C. Sequences were aligned using MULTALIGN (*45*). Identical amino acids are shaded black, and italics denote substitutions of nonsimilar amino acids. Rows are ordered by similarity. Proteins included in the alignment are NCIB10662 (C) [*C. perfringens* strain NCIB10662 (type C) alpha-toxin (Genbank accession number D10248)], CER89L43 [*C. perfringens* strain CER89L43 alpha-toxin (L43545)], NCTC8237 [*C. perfringens* strain NCTC8237 alpha-toxin (X13608)], strain 8-6 [*C. perfringens* strain 8-6 alpha-toxin (X17300)], SWCP [*C. perfringens* strain SWCP alpha-toxin (AF204209)], cnov [*C. novyi* PLC (D32125)], and cbif [*C. bifermantans* PLC (AF072123)].

Crystal Structure of Strain SWCP Alpha-Toxin. The final model built into the electron density map contains two SWCP alpha-toxin molecules, each consisting of 2995 protein atoms. Each protein molecule had three bound zinc atoms (Figure 3), and in addition, the asymmetric unit contained 152 water molecules. The final *R*-factor and R_{free} were 20.7 and 24.2%, respectively. Statistics for the final model are given in Table 1. The majority of the residues have well-defined electron density (Figure 4), and in regions of poorer density (loop

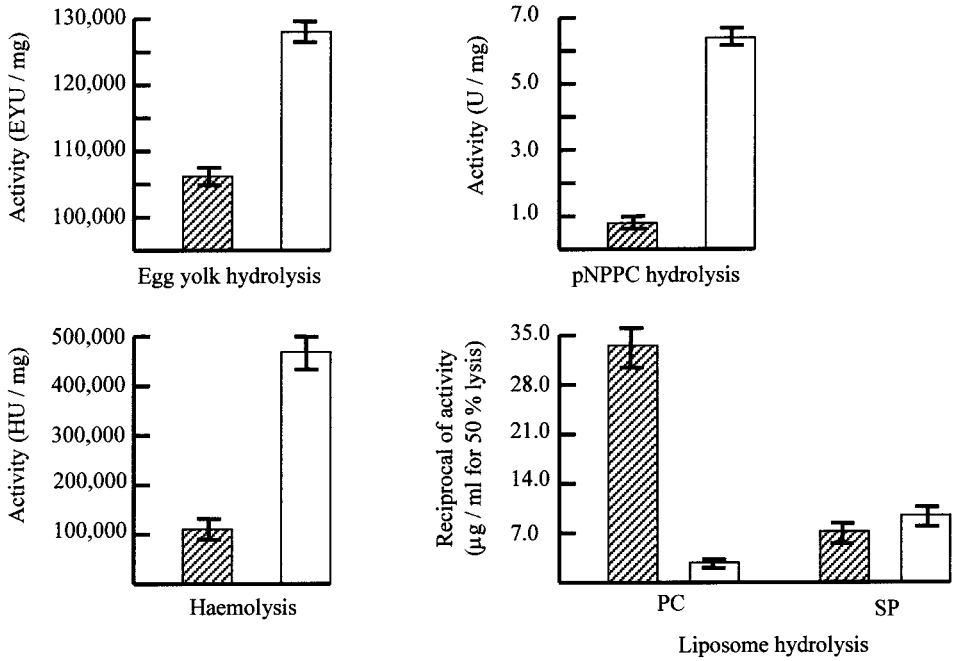

FIGURE 2: Activities of SWCP (cross-hatched columns) and NCTC8237 (white columns) alpha-toxins. For the egg yolk hydrolysis assay, 10 μg/mL SWCP and NCTC8237 toxin were used (*24*). For the ρNPPC hydrolysis assay, 200 μg/mL SWCP and 40 μg/mL NCTC8237 toxin were used. One unit hydrolyzes 1 nmol of ρNPPC in 1 min at 37 °C. The hemolysis assay used 10 μg/mL SWCP and NCTC8237 toxin. HU represents hemolytic units (*24*). The liposome hydrolysis assay used 10 μg/mL SWCP and 40 μg/mL NCTC8237 toxin for the phosphatidylcholine (PC) liposomes and both toxins at 40 μg/mL for the sphingomyelin (SP) liposomes. All experiments were carried out for 1 h at 37 °C. The results that are shown are the means of six separate experiments with SE bars.

residues 79−85 and linker residues 244−247), it is still possible to trace the polypeptide chain. The model has good stereochemistry (see Table 1), and the geometry of the residues is better than expected for the average 2.4 Å structure according to PROCHECK (*36*) analyses. Of all the residues built into both chains, 91.5% lie within the most favored region, and there is only one residue (Ser A250) out of the 740 that lies in the disallowed region. The two SWCP protein molecules are related by a noncrystallographic 2-fold axis parallel to the diagonals of the *ab* plane of the unit cell. A number of large hydrophobics that are exposed on the membrane binding surface of alpha-toxin are assumed to anchor the toxin in the cell membrane and are buried in the interface between the two noncrystallographic molecules. Interestingly, this includes a π-stacking interaction between the two aromatic rings of Phe 84 in the molecule and its ncs mate. A similar but not identical membrane-binding surface packing has also been observed between the crystallographically related molecules in the open-form crystal structure (*11*). This interaction did not include the stacking of Phe 84 as this residue is disordered in the open-form structure (*11*). The two molecules in the asymmetric unit are nearly identical (the all-atom rms deviation is just 0.7 Å when the two molecules are optimally superimposed). We will therefore be referring to molecule A only for the remainder of this paper.

Overall, the three-dimensional structure of SWCP alpha-toxin is similar to the previously determined structures of CER89L43 alpha-toxin (Figure 3), and in particular to the open conformation (*11*). This could be expected as the sequences of the two proteins are 80% identical. It can be classified as an open form of the enzyme; there are three zinc ions in the active site, which is accessible to substrate. The overall structure is conserved with the N-terminal domain being helical and the C-terminal domain consisting of an eight-stranded antiparallel β-sandwich with an immunoglobulin-like fold. If the C-terminal domain of the SWCP alpha-toxin is optimally superimposed on that of the CER89L43 open form, the rmsd for all main chain atoms in this domain is 1.1 Å. In contrast, when the N-terminal domains of these two structures are superimposed, then the rmsd for all main chain atoms is 2.8 Å. However, when residues 75−86, which were disordered in the open CER89L43 structure, are excluded from the comparison, the rmsd for the main chain atoms of the N-terminal domain drops to only 0.67 Å.

Metal Ion Binding by SWCP Alpha-Toxin. Each of the two molecules in the asymmetric unit had three zinc atoms (Zn1, Zn2, and Zn3) in the active site. The *B*-factors for these zinc atoms (26.5, 27.3, and 31.1 Å^2, respectively, for molecule A of the ASU) are similar to the average *B*-factors of the protein (molecule A has average main chain and side chain *B*-factors of 32.2 and 33.4 Å^2, respectively), indicating that the sites are probably fully occupied. The average bond length for zinc coordination was 2.35 Å, which is typical for zinc−protein interactions. Zn1 is coordinated by Trp 1, Asp 130, and His 11, Zn2 (Cd3 in the open-form structure; *11*) by Asp 56, His 68, His 126, and Asp 130, and Zn3 (Cd2 in the open-form structure; *11*) by His 136, His 148, Glu 152, and Wat 1. These residues are all essential for the catalytic activity of alpha-toxin (*37*−*39*).

The zinc ion binding in SWCP alpha-toxin contrasts with that seen in either the open- or closed-form CER89L43 structure. The active site of the closed form of the CER89L43 toxin contains two zinc ions (Zn1 and Zn2). Three metal ions were seen in the active site of the open form of the CER89L43 toxin, with protein ligands identical to those for the SWCP toxin. However, the crystallization buffer for the

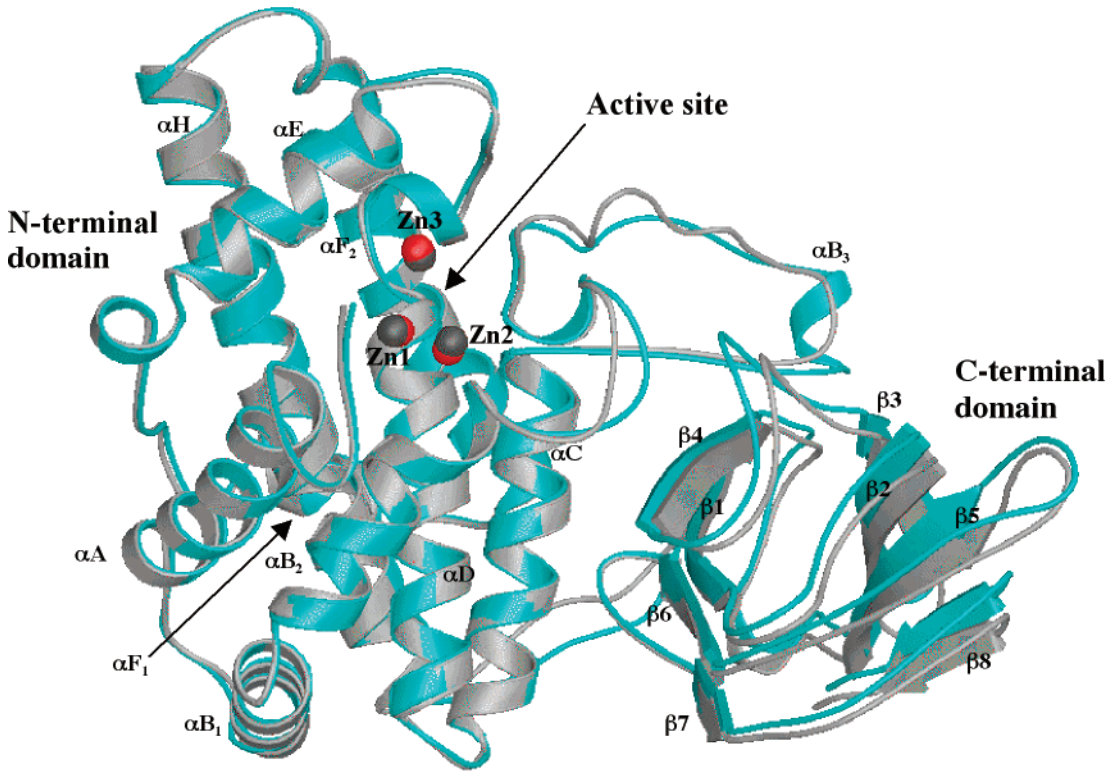

FIGURE 3: Superposition of SWCP (blue) and CER89L43 (gray) alpha-toxins. The N-terminal domains have been superposed. The SWCP active site zinc ions are colored red, and the CER89L43 active site divalent cations are colored dark gray. This figure, and all the other structural illustrations, was drawn using Bobscript (*47*), a modification of Molscript (*48*), and subsequently rendered with Raster3D (*49*, *50*).

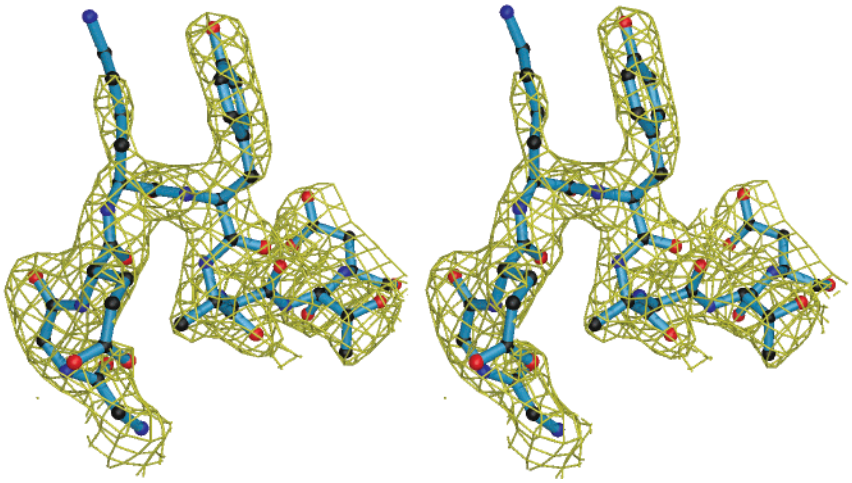

FIGURE 4: Stereoview of the final $2F_o - F_c$ electron density map, contoured at the 1σ level around residues 265−273.

open form of the CER89L43 toxin contained 50 mM cadmium sulfate (*40*). As a result, two of the three sites are occupied by cadmium ions (which can act as a zinc ion analogue). In addition, 10 cadmium ions were observed bound, predominantly nonspecifically, to the protein surface (*11*). These surface-bound divalent cations were absent in the SWCP structure.

The SWCP Alpha-Toxin Exhibits Differences from the CER89L43 Alpha-Toxin in Putative Membrane Recognition Regions. The amino acid sequence differences that exist between the SWCP alpha-toxin and the alpha-toxins from other strains of *C. perfringens* are distributed randomly throughout the protein. None of the differences occur in the active site, though substitutions do occur in regions of the protein thought to play a key role in membrane−protein interactions. Three calcium ions have been shown crystallographically to bind to the C-terminal domain of the closed form of the NCTC8237 alpha-toxin (*16*). On the basis of site-specific modification of the their associated protein ligands, these calcium ions have been shown to be important for activity (*17*, *18*). Since these ions are all found in the proposed membrane-binding plane of the C-terminal domain (*11*), but with incomplete coordination, it is thought that they contribute to membrane binding by interacting with both the protein and the phosphate moiety of membrane phospholipids. The binding site for one of these calcium ions, Ca1, consists of Asp 336 Od2, Asp 269 O, Gly 271 O, and Ala 337 O. In SWCP alpha-toxin, there are two changes (A337D

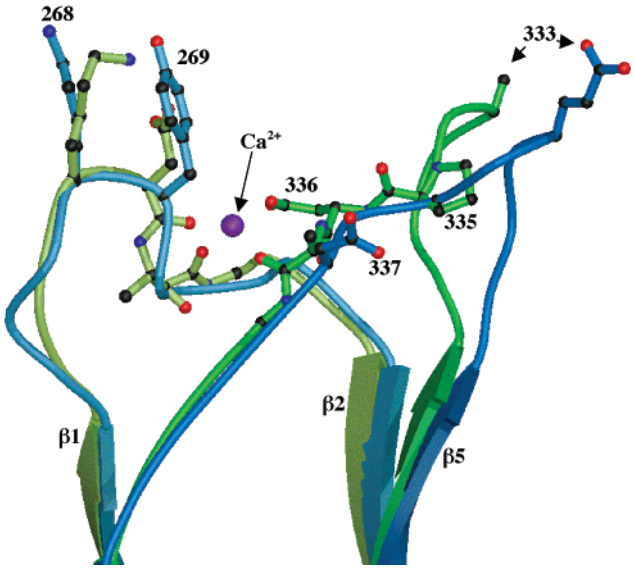

FIGURE 5: Superposition of the calcium binding pocket of SWCP (blue) and CER89L43 (green) alpha-toxins. The pocket is formed by residues 265−272 and 330−338, with the calcium ion coordinated by residues 269, 271, 336, and 337 (shown in ball-and-stick representation for the CER89L43 structure). The calcium ion is chown for the CER89L43 structure only. Residues that differ between the two structures are shown in ball-and-stick representation.

and D269Y) occurring directly in this binding pocket and two changes in the associated loop (A333D and P335G). Figure 5 shows a superposition of the open-form CER89L43 and SWCP structures in this area, and it can be seen that the local interactions and, in particular, the overall conformation of residues 330−337 differ markedly. It is interesting to note from this illustration that the position of the side chain of D337 in the binding pocket of the SWCP structure means that it may exactly replace that of D269 in the CER89L43 structure. The difference in the conformation of residues 330−337 between the SWCP and CER89L43 open-form toxins (rmsd for all main chain atoms between these residues of 2.2 Å) may be the result of the substitution of proline 335 in CER89L43 for glycine in the SWCP structure and the consequent increase in backbone flexibility. However, conformational flexibility has been noted in this loop previously (*12*), with the open- and closed-form alpha-toxins showing divergent conformations (the main chain atom rmsd between the two structures is 1.3 Å).

The observed conformational flexibility of this loop is apparently not due to the effects of divalent ion binding to the C domain, but may be due to its inherent flexibility. The structures of SWCP and closed-form CER89L43 toxins, neither of which had divalent cations bound to their C domains, are more dissimilar from one another (having a main chain rmsd of 2.4 Å) than either is from the open CER89L43 toxin structure, which has cadmium ion bound to this site. In addition, the calcium-bound closed form of NCTC8237 has a conformation identical to that of the CER89L43 calcium-free closed structure in this loop.

Interactions between the N and C Domains Are Dissimilar in the SWCP and CER89L43 Alpha-Toxin Structures. There are four other regions where the SWCP and CER89L43 or NCTC8237 proteins differ in their backbone traces. Residues 59−62, and 294 and 295, have average main chain rms difference values of 2.5 and 2.0 Å, respectively. These residues form an interaction between the N- and C-terminal domains in the SWCP toxin with a H-bond between Ala 61 (O) and Gly 296 (N) (bond length of 2.7 Å). This interaction does not occur in the strain CER89L43 structure (open form) as amino acids 60−62 are flipped away from the C-terminal domain and Ala 61 (O) is 9.0 Å away from Gly 296 (N). Residues 59−67 are disordered in the closed-form CER89L43 structure. However, they are ordered in the calcium-bound closed form of the NCTC8237 alpha-toxin, and adopt a conformation quite different from that seen in the CER89L43 open-form and SWCP toxins (which are basically identical with the exception of residues 60−62) (*16*). Interestingly, in the CER89L43 closed form, residues 60−62 still interact with the C-terminal domain, specifically, via hydrogen bonds between Tyr 62 Oη and Asn 294 Nδ2 and also Thr 306 O and N, and Tyr 62 O and Asn 297 N.

Residues 72−90 are part of a loop that travels in a direction away from the N-terminal domain toward the C-terminal domain (Figure 3). There is a small 3_{10}-helix (αB_3) in the SWCP structure formed by residues 83−86 which is not present in any previously reported structure of alpha-toxin. After this helix, the loop interacts with the C-terminal domain (H-bond between Ile 90 N and Thr 308 CO) before running back toward the N-terminal domain. The optimally superposed N-terminal domains of SWCP and open-form CER89L43 toxins for residues 75−86 have an all-atom rmsd of 12.5 Å. However, given the highly disordered nature of the majority of this loop in the CER89L43 open-form structure, it is possible that the CER89L43 toxin could adopt the same conformation as SWCP. In contrast, these residues are well-ordered in the closed form but adopt a completely different conformation (*12*); a helix is formed, but this time from residues 73−80 (labeled αB_2 in ref *12*), and αB_3 is absent. This closed-form conformation is associated with the additional loop movements (residues 132−145) that result in the active site being obscured and the destruction of the third zinc site already alluded to, while both the SWCP and CER89L43 open conformations allow the active site to be accessible to substrate and to contain three zinc ions.

DISCUSSION

The alpha-toxin from *C. perfringens* strain SWCP has 58 amino acid differences when compared with the alpha-toxin from *C. perfringens* strain CER89L43 and 57 amino acid differences with that from strain NCTC8237; the SWCP protein differs by 16−18% when compared with all of the other alpha-toxin sequences reported to date, which are available in GenBank (see the legends of Figures 1 and 6). It is by far the most divergent of the *C. perfringens* alpha-toxins characterized to date. A multiple-sequence alignment of SWCP alpha-toxin, a representative group of previously sequenced alpha-toxins from different *C. perfringens* strains, and the *C. bifermentans*, *C. novyi*, and *B. cereus* phospholipases C was carried out using ClustalW (*41*) (Figure 6). Subjecting this alignment to bootstrapping analysis showed that the SWCP toxin was always placed on a branch of the tree separate from the other alpha-toxin variants, but was always more related to these than any of the other phospholipases C that were included. It is likely that the sequence of SWCP toxin is so divergent from those previously

a

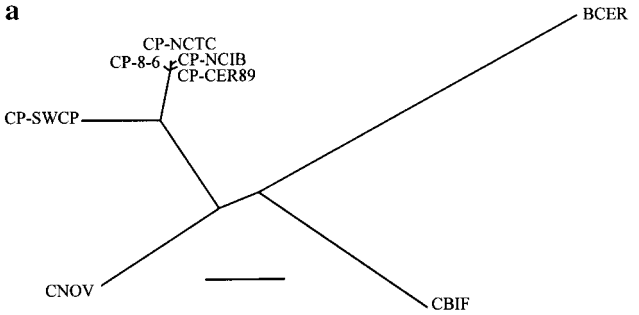

b

	CP-NCTC	CP-CER89	CP-SWCP	CNOV	CBIF
BCER	16.6	16.6	19.0	19.3	19.5
CBIF	53.0	52.7	52.4	54.3	
CNOV	61.6	61.9	61.4		
CP-SWCP	84.3	84.3			
CP-CER89	98.9				

FIGURE 6: (a) Radial rootless phylogenetic tree of bacterial phosphatidylcholine-specific phospholipases C. The phylogenetic order was calculated using ClustalW (*41*) and visualized using TreeView (*51*). Branch length represents the evolutionary distance between proteins with the scale bar representing a substitution of 30 amino acids. (b) Levels of sequence identity between bacterial phosphatidylcholine-specific phospholipases C (in percentages). BCER, *B. cereus* PLC; CBIF, *C. bifermentans* PLC; CNOV, *C. novyi* PLC; CP-SWCP, *C. perfringens* strain SWCP alpha-toxin; CP-8-6, *C. perfringens* strain 8-6 alpha-toxin; CP-NCTC, *C. perfringens* strain NCTC8237 alpha-toxin; CP-CER89, *C. perfringens* strain CER89L43 alpha-toxin; and CP-NCIB, *C. perfringens* strain NCIB10662 alpha-toxin. GenBank accession numbers are X12854 (BCER), AF072123 (CBIF), D32125 (CNOV), AF204209 (CP-SWCP), X17300 (CP-8-6), X13608 (CP-NCTC), L43545 (CP-CER89), and D10248 (CP-NCIB).

characterized because of its source; the SWCP strain was isolated from an avian species, and all the others originate from mammals. Since the phospholipid composition of cellular membranes varies between hosts, this alpha-toxin may have evolved to be most effective in an avian host. In support of this hypothesis, we have shown in this paper that the turnover rate of different substrates differed between the SWCP toxin and the NCTC8237 alpha-toxins. No other *cpa* genes from avian strains have been characterized, so it is impossible to conclude that such divergent sequences are common to all isolates from birds. However, the divergence of SWCP from other alpha-toxin sequences is larger in magnitude than that observed in some cases for the same protein from different but related species, and so our findings have implications for the development of antibody or PCR-based diagnostic tests for the *C. perfringens* alpha-toxin or for the *cpa* gene, and for the development of vaccines to protect against necrotic enteritis in chickens.

Figure 7 shows the residue-by-residue main chain rmsd between these two structures, with the N-terminal and C-terminal domains superimposed separately. The overall structure of SWCP alpha-toxin showed that the active site remained unchanged compared to the CER89L43 open-form structure and the backbone trace is almost identical in most regions of the protein. However, there were conformational differences in some parts of the chain. Clearly, it would be interesting to relate these conformational changes to the altered substrate specificity that our kinetic studies revealed.

We believe one of the most significant differences described in the Results is around the calcium-binding pocket formed by residues 269, 271, 336, and 337 (Figure 5);

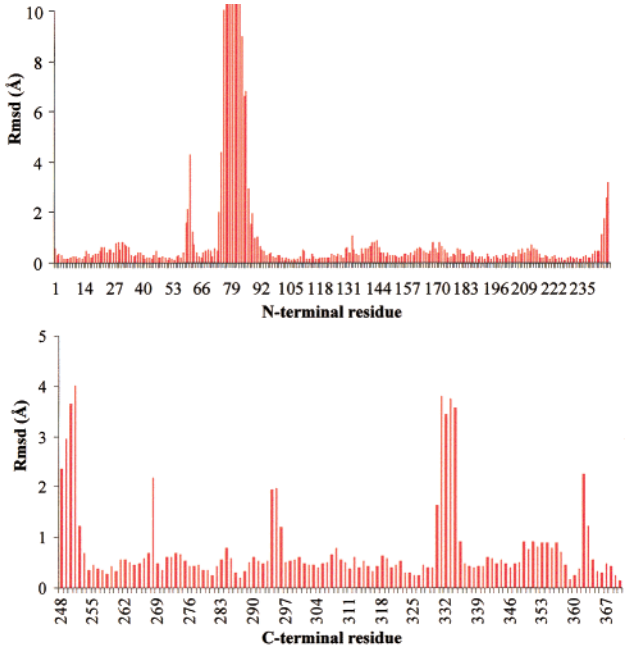

FIGURE 7: Residue-by-residue root-mean-square differences between the individually aligned N- and C-terminal domains of SWCP and CER89L89 open-form alpha-toxins.

neutralizing monoclonal antibodies bind to this region (*10*), inhibit alpha-toxin activity, and may block membrane−protein interactions. A calcium ion has been crystallographically observed bound to this pocket in the closed-form NCTC8237 structure (*16*), while in the open form, a cadmium ion is bound (*11*). In the SWCP structure, this metal ion was replaced with a water molecule (there were no divalent cations under the crystallization conditions). As already noted, although the binding site itself is conserved, there are a number of amino acid substitutions (D269Y, P335G, and A337D), and the conformation of residues 330−337 is markedly different between the NCTC8237 and SWCP toxins. It is tempting to link changes in this region with the differing substrate preferences between the two proteins; the ratio of phosphatidylcholine to sphingomyelin activity is 0.41 for NCTC8237 alpha-toxin and 4.9 for SWCP alpha-toxin. This may be explained by the addition of a large hydrophobic residue (Tyr 269) to the binding region in the SWCP toxin. It has been postulated that sphingomyelin packs with an increased density in the hydrophobic core of a membrane (compared to phosphatidylcholine), and such packing could hinder the insertion of large residues. This hypothesis was previously reported to explain the lower affinity of the calcium−phospholipid binding domain from cytosolic phospholipase A2 for sphingomyelin membranes (*42*, *43*). Site-directed mutagenesis experiments on alpha-toxin in this area of the protein should help to verify some of the determinants of substrate specificity for these enzymes. SWCP toxin is also less active against ρNPPC than NCTC8237 toxin, but since this substrate is not membrane-bound, mutations in the C-terminal domain cannot be responsible for this difference in activity.

Another difference between the two proteins is in the region spanning residues 72−90. The chain trace of loop residues 72−82 varies considerably between the two structures, and in the strain SWCP structure, there is a small 3_{10}-helix formed by residues 83−86 (Figure 3). The electron

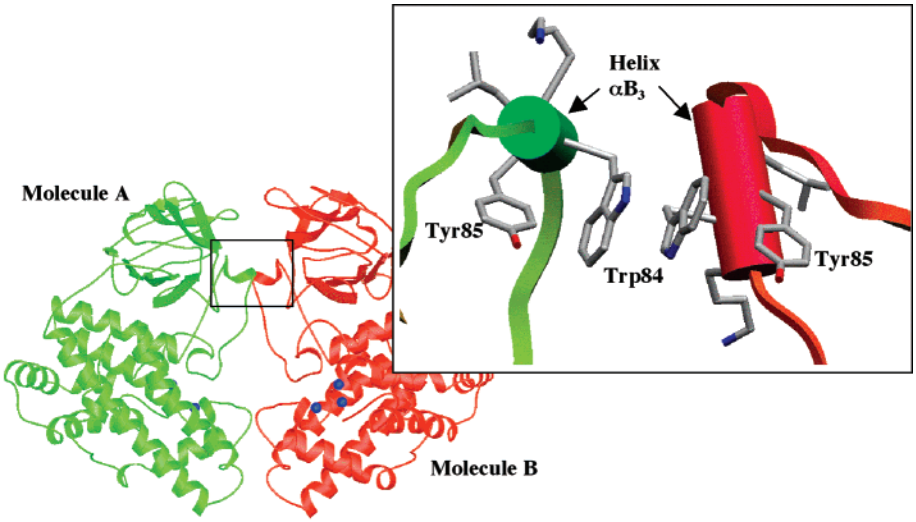

FIGURE 8: Stabilization of the αB_3 helix via an aromatic $\pi-\pi$ stacking interaction between the two noncrystallographically related molecules in the asymmetric unit. Molecule A is colored green, and molecule B is colored red. The inset shows an enlarged view of the helices, which are represented by cylinders. The main picture was drawn with Bobscript and rendered with Raster3D, and the inset was drawn using SETOR (*52*).

density is good for this region, and the helix is well-ordered with average *B*-factors for the residues of 24.2 Å^2. It is stabilized by interactions with its noncrystallographic symmetry-related copy (Figure 8); Trp 84 from molecule A and molecule B form a $\pi-\pi$ aromatic stacking interaction. This is the first example of residues 84−88 being ordered in an open form of alpha-toxin. It is possible that this is the conformation of the loop present in other open-form alpha-toxins. However, there are three mutations between the SWCP and CER89L43 toxin sequences in the residues that are near or part of the helix. Residues 79−86 are **T**KD-**SK**WYL in the SWCP sequence and **S**KD**NS**WYL in CER89L43. In addition, this loop is one of the two that undergoes a change in conformation between the open and closed forms of CER89L43 alpha-toxin, and we have previously hypothesized that the opening and closing of the active site is associated with membrane recognition (*12*, *16*). The loop sits on the membrane binding surface of the protein (Figure 3), and contains a number of hydrophobic residues that may be expected to be involved in membrane recognition.

Finally, the discovery of three zinc ions in an active site that is open and accessible to solvent is of interest. Since no divalent cations were added to the crystallization buffer, this result suggests that the protein can retain sufficient zinc ions during purification to allow a population to crystallize with three zinc ions in the active site. The CER89L43 closed form was also crystallized in the absence of any added divalent cations (*40*), but in this case, the toxin in the crystals contained only two zinc ions. The question of why SWCP crystallized with three zinc ions arises, whereas the CER89L43 closed form contains only two zinc ions. One possible answer is that the closed-form crystallization conditions are high in salt (1.8−2.0 M NaCl), while the SWCP toxin crystallized from conditions that include lower salt concentrations and organic solvent. Perhaps, therefore, the SWCP conditions reflect an environment in which the open form is stabilized, while the CER89L43 closed-form crystallization conditions reflect the response of the enzyme to the high-salt conditions.

In conclusion, we have characterized an alpha-toxin from a strain of *C. perfringens* isolated from a diseased swan. The sequence of this alpha-toxin was highly divergent from those of alpha-toxins produced by other *C. perfringens* strains. The SWCP toxin had significantly altered substrate specificity, when compared to another typical *C. perfringens* alpha-toxin. The crystal structure revealed some interesting differences between SWCP alpha-toxin and the previously determined structures of alpha-toxin from *C. perfringens* strain CER89L43. These differences were in areas of the protein which have been shown to be important for activity, in particular around residues 330−337, and also in regions of known conformational flexibility (residues 72−90). Finally, we have related these sequence and structural changes to the changes in substrate specificity, and thus gained insight into the mechanism of action and membrane binding of the protein. We were also able to suggest that the reason for the diversity lies in the unusual origin of the protein.

Such information about sequence and structural variation, particularly when linked to changes in enzymatic activity and specificity, is essential when developing an effective vaccine that will protect a wide range of important domestic livestock. Such a vaccine would, for example, be more valuable if it is able to protect both cattle from sudden death and chickens from necrotic enteritis. Previous work has shown that the protective antibody response to alpha-toxin is directed against the C-terminal domain of the protein (*44*), but the locations of epitopes in this domain have not been determined. Our data show that the C-terminal domain of the alpha-toxin from an avian isolate is folded in a manner similar to that of the C-terminal domain of alpha-toxin from human and bovine sources (*11*, *12*, *16*). However, our finding that surface-exposed residues in the C-terminal domain of the SWCP alpha-toxin are not identical with their counterparts in the human and bovine proteins indicates that these domains may not be immunologically identical. This might have implications for the ability of a vaccine to provide protection against all forms of alpha-toxin. In addition, further work is also required to establish whether other avian isolates

of *C. perfringens*, including those isolated from chickens suffering from necrotic enteritis, produce a protein which is more similar to the SWCP alpha-toxin or to the alpha-toxins produced by *C. perfringens* isolated from cases of disease in mammals.

ACKNOWLEDGMENT

We thank Dr. J. Clapperton and Dr. J. Eaton and the staff at the SRS, CCLRC Daresbury Laboratory, for their support during data collection.

REFERENCES

1. Macfarlane, M. G., and Knight, B. C. J. G. (1941) *Biochem. J. 42*, 587−590.
2. Titball, R. W. (1993) *Microbiol. Rev. 57*, 347−366.
3. Titball, R. W., Naylor, C. E., and Basak, A. K. (1999) *Anaerobe 5*, 51−64.
4. Awad, M. M., Bryant, A. E., Stevens, D. L., and Rood, J. I. (1995) *Mol. Microbiol. 15*, 191−202.
5. Murrell, W. G., Stewart, B. J., O'Neill, C., Siarakas, S., and Kariks, S. (1993) *J. Med. Microbiol. 39*, 114−127.
6. Siarakas, S., Damas, E., and Murrell, W. G. (1997) *Pathology 29*, 278−285.
7. Baba, E., Fuller, A. L., Gilbert, J. M., Thayer, S. G., and McDougald, L. R. (1992) *Avian Dis. 36*, 59−62.
8. Cygan, Z., and Buczek, J. (1993) *Med. Weter. 49*, 469−471.
9. Elwinger, K., and Teglof, B. (1991) *Arch. Gefluegelkd. 55*, 69−73.
10. Ginter, A., Williamson, E. D., Dessy, F., Coppe, P., Bullifent, H., Howells, A., and Titball, R. W. (1996) *Microbiology 142*, 191−198.
11. Naylor, C. E., Eaton, J. T., Howells, A., Justin, N., Moss, D. S., Titball, R. W., and Basak, A. K. (1998) *Nat. Struct. Biol. 5*, 738−746.
12. Eaton, J. T., Naylor, C. E., Howells, A., Moss, D. S., Titball, R. W., and Basak, A. K. (2001) *J. Mol. Biol.* (submitted for publication).
13. Titball, R. W., Leslie, D. L., Harvey, S., and Kelly, D. (1991) *Infect. Immun. 59*, 1872−1874.
14. Nagahama, M., Michiue, K., Mukai, M., Ochi, S., and Sakurai, J. (1998) *Microbiol. Immunol. 42*, 533−538.
15. Nalefski, E. A., and Falke, J. J. (1996) *Protein Sci. 5*, 2375−2390.
16. Naylor, C. E., Jepson, M., Crane, D. T., Titball, R. W., Miller, J., Basak, A. K., and Bolgiano, B. (1999) *J. Mol. Biol. 294*, 757−770.
17. Alape-Giron, A., Flores-Diaz, M., Guillouard, I., Naylor, C. E., Titball, R. W., Rucavado, A., Lomonte, B., Basak, A. K., Gutierrez, J. M., Cole, S. T., and Thelestam, M. (2000) *Eur. J. Biochem. 267*, 5191−5197.
18. Guillouard, I., Alzari, P. M., Saliou, B., and Cole, S. T. (1997) *Mol. Microbiol. 26*, 867−876.
19. Krug, E. L., and Kent, C. (1984) *Arch. Biochem. Biophys. 231*, 400−410.
20. Young, P. R., Snyder, W. R., and McMahon, R. F. (1991) *Biochem. J. 280*, 407−410.
21. Tso, J. Y., and Siebel, C. (1989) *Infect. Immun. 57*, 468−476.
22. Van Damme-Jongsten, M., Wernars, K., and Notermans, S. (1989) *Antonie Van Leeuwenhoek 56*, 181−190.
23. Sambrook, J., Fritsch, E. F., and Maniatis, T. (1989) *Molecular cloning: a laboratory manual*, 2nd ed., Cold Spring Harbor Laboratory Press, Plainview, NY.
24. Titball, R. W., Hunter, S. E., Martin, K. L., Morris, B. C., Shuttleworth, A. D., Rubidge, T., Anderson, D. W., and Kelly, D. C. (1989) *Infect. Immun. 57*, 367−376.
25. Basak, A. K., Stuart, D. I., Nikura, T., Bishop, D. H., Kelly, D. C., Fearn, A., and Titball, R. W. (1994) *J. Mol. Biol. 244*, 648−650.
26. Senior, J., Gregoriadis, G., and Mitropoulos, K. A. (1983) *Biochim. Biophys. Acta 760*, 111−118.
27. Garman, E. F., and Schneider, T. R. (1997) *J. Appl. Crystallogr. 30*, 211−237.
28. Otwinowski, Z., and Minor, W. (1997) *Methods Enzymol. 276*, 307−326.
29. Collaborative Computation Project No. 4 (1994) *Acta Crystallogr. D50*, 760−763.
30. Evans, P. R. (1997) in *CCP4 Study Weekend on Recent Advances in Phasing* (Wilson, K. S., Davies, G., Ashton, A. W., and Bailey, S., Eds.) pp 97−102, CCLRC, Daresbury Laboratory, Warrington, U.K.
31. Navaza, J. (1994) *Acta Crystallogr. A50*, 157−163.
32. Cowtan, K. (1994) *Joint CCP4 and ESF-EACBM Newsletter on Protein Crystallography 31*, 34−38.
33. Read, R. J. (1986) *Acta Crystallogr. A42*, 140−149.
34. Jones, T. A., and Kjelgaard, M. (1997) *Methods Enzymol. 277*, 173−208.
35. Brunger, A. T. (1992) *X-PLOR version 3.1. A system for X-ray crystallography and NMR*, Yale University Press, New Haven, CT.
36. Laskowski, R. A., MacArthur, M. W., Moss, D. S., and Thornton, J. M. (1993) *J. Appl. Crystallogr. 26*, 283−291.
37. Nagahama, M., Nakayama, T., Michiue, K., and Sakurai, J. (1997) *Infect. Immun. 65*, 3489−3492.
38. Nagahama, M., Okagawa, Y., Nakayama, T., Nishioka, E., and Sakurai, J. (1995) *J. Bacteriol. 177*, 1179−1185.
39. Guillouard, I., Garnier, T., and Cole, S. T. (1996) *Infect. Immun. 64*, 2440−2444.
40. Basak, A. K., Howells, A., Eaton, J. T., Moss, D. S., Naylor, C. E., Miller, J., and Titball, R. W. (1998) *Acta Crystallogr. D54*, 1425−1428.
41. Thompson, J. D., Higgins, D. G., and Gibson, T. J. (1994) *Nucleic Acids Res. 22*, 4673−4680.
42. Perisic, O., Fong, S., Lynch, D. E., Bycroft, M., and Williams, R. L. (1998) *J. Biol. Chem. 273*, 1596−1604.
43. Perisic, O., Paterson, H. F., Mosedale, G., Lara-Gonzalez, S., and Williams, R. L. (1999) *J. Biol. Chem. 274*, 14979−14987.
44. Williamson, E. D., and Titball, R. W. (1993) *Vaccine 11*, 1253−1258.
45. Barton, G. J. (1990) *Methods Enzymol. 183*, 403−428.
46. Laemmli, U. K. (1970) *Nature 227*, 680−685.
47. Esnouf, R. (1997) *J. Mol. Graphics 15*, 132−134.
48. Kraulis, P. (1991) *J. Appl. Crystallogr. 24*, 946−950.
49. Merritt, E. A., and Murphy, M. E. P. (1994) *Acta Crystallogr. D50*, 869−873.
50. Bacon, D. J., and Anderson, W. F. (1988) *J. Mol. Graphics 6*, 219−220.
51. Page, R. D. M. (1996) *CABIOS, Comput. Appl. Biosci. 12*, 357−358.
52. Evans, S. V. (1993) *J. Mol. Graphics 11*, 134−138.

BI012015V